Journal of Radiation Research and Applied Sciences 16 (2023) 100607

Contents lists available at ScienceDirect

Journal of Radiation Research and Applied Sciences

journal homepage: www.journals.elsevier.com/journal-of-radiation-research-and-applied-sciences

Epileptic seizure detection from electroencephalogram (EEG) signals using linear graph convolutional network and DenseNet based hybrid framework

Ferdaus Anam Jibon [a], Mahadi Hasan Miraz [b], Mayeen Uddin Khandaker [c,d,*], Mostafa Rashdan [e], Mohammad Salman [e], Alif Tasbir [a], Nazibul Hasan Nishar [a], Fazlul Hasan Siddiqui [f]

[a] Department of Computer Science & Engineering, University of Information Technology & Sciences (UITS), Dhaka, Bangladesh
[b] Department of Management, Marketing and Digital Business, Faculty of Business, Curtin University Malaysia, Malaysia
[c] Centre for Applied Physics and Radiation Technologies, School of Engineering and Technology, Sunway University, Bandar Sunway, 47500, Selangor, Malaysia
[d] Department of General Educational Development, Faculty of Science and Information Technology, Daffodil International University, DIU Rd, Dhaka, 1341, Bangladesh
[e] College of Engineering and Technology, American University of the Middle East, Kuwait
[f] Department of Computer Science & Engineering, Dhaka University of Engineering & Technology (DUET), Gazipur, Bangladesh

ARTICLE INFO

Keywords:
Linear graph convolutional network (LGCN)
DenseNet
Stockwell transformation (S-transform)
Hybrid model
Electroencephalogram (EEG) signal
Seizure detection
CHB-MIT Dataset

ABSTRACT

A clinical condition known as epilepsy occurs when the brain's regular electrical activity is disturbed, resulting in a rapid, aberrant, and excessive discharge of brain neurons. The electroencephalogram (EEG) signal is the measurement of electrical activity received from the nerve cells of the cerebral cortex to make precise diagnoses of disorders, which is made crucial attention for treating epilepsy patients in recent years. The concentration on grid-like data has been a significant drawback of existing deep learning-based automatic epileptic seizure detection algorithms from raw EEG signals; nevertheless, physiological recordings frequently have irregular and unordered structures, making it challenging to think of them as a matrix. In order to take advantage of the implicit information that exists in seizure detection, graph neural networks have received a lot of attention. These networks feature interacting nodes connected by edges whose weights can be either dictated by temporal correlations or anatomical junctions. To address this limitation, a novel hybrid framework is proposed for epileptic seizure detection by using linear graph convolution neural network (LGCN) and DenseNet. When compared to previous deep learning networks, DenseNet achieves the model's higher computational accuracy and memory efficiency by reducing the vanishing gradient problem and enhancing feature propagation in each of its layers. The Stockwell transform (S-transform) is used to preprocess from the raw EEG signal and then group the resulting matrix into time-frequency blocks as inputs for the LGCN to use for feature selection and after the Densenet uses for classification. The proposed hybrid framework outperforms the state-of-the-art in seizure detection tasks, achieving 98% accuracy and 98.60% specificity in extensive experiments on the publicly available CHB-MIT EEG dataset.

1. Introduction

A network of different nerve cells or neurons makes up the human nervous system. To communicate with nerve cells, brain cells produce electrical impulses. For a healthy brain, these impulses follow a typical pattern. The normal transmission of information throughout the body is disrupted by any injury or damage to this network of neurons. Neurological diseases are the general term used to describe these anomalies. Neurological disorders include common ones including epilepsy, brain tumors, Parkinson's disease, stroke, and others (Eftekhar, Juffali, El-Imad, Constandinou, Toumazou). Epilepsy ranks as the fourth most prevalent neurological condition affecting the brain's central nervous system. Patients with epilepsy occasionally experience unexpected changes in their electrical impulses as a result of excessive

* Corresponding author. Centre for Applied Physics and Radiation Technologies, School of Engineering and Technology, Sunway University, Bandar Sunway, 47500, Selangor, Malaysia.
E-mail addresses: ferdaus.anam@uits.edu.bd (F.A. Jibon), Mahadi.miraz@curtin.edu.my (M.H. Miraz), mu_khandaker@yahoo.com, mayeenk@sunway.edu.my (M.U. Khandaker), mostafa.rashdan@aum.edu.kw (M. Rashdan), mohammad.salman@aum.edu.kw (M. Salman), aliftasbir@gmail.com (A. Tasbir), nazibulhasan98@gmail.com (N.H. Nishar), siddiqui@duet.ac.bd (F.H. Siddiqui).

https://doi.org/10.1016/j.jrras.2023.100607
Received 26 February 2023; Received in revised form 16 May 2023; Accepted 19 May 2023
Available online 24 May 2023

electrical discharge. Patients lose consciousness or awareness as a result of the brain becoming unstable. Seizures are characterized by this unsteady state. A seizure may result in several different kinds of injury. Epilepsy is a condition that affects 1% of people worldwide. Some transient electric problems affect epileptic seizure patients. One or more strokes occur in a month for about 20–30 percent of people with epilepsy. Physical harm could potentially result in the patient's death during the duration of epileptic seizures (Sharif, Jafari).

A variety of factors make EEG a potent method for examining brain activity. The ability of EEGs to detect changes over milliseconds is good given that an action potential can travel through a single neuron in anywhere between 0.5 and 130 ms depending on the type of neuron. Other methods used to study brain activity include fMRI, PET, and fUS, which have time resolutions ranging from seconds to minutes. According to accepted clinical recording methods, activity below or above this range is likely to be artifactual because this is where the majority of the brain signal detected by the scalp EEG lies. The majority of EEGs used in clinical practice are divided into waveform bandwidths designated alpha, beta, theta, and delta. Some people divide the bands into subbands to facilitate data analysis (Boonyakitanont, Lek-uthai, Chomtho, Songsiri).

Manually observing and diagnosing epileptic convulsions by a neurologist is laborious, time-consuming, and prone to mistakes. In order to reduce the number of lengthy EEG recordings that need to be evaluated by neurologists, it is crucial to build an automatic computer-aided (CAD) system to assist neurologists and patients in identifying and detecting epileptic seizures. Signal acquisition, data preprocessing, feature extraction, channel selection, classification, and performance analysis/decision making are a few of the processes for epileptic seizure detection using EEG analysis that are required to construct an autonomous CAD system. It is necessary to extract appropriate and useful features for classifiers to distinguish and describe various epileptic seizures due to the complicated morphology of the EEG data and the visual resemblance between epileptic and normal signals (Saminu et al., 2021). Table 1 Shows the various band frequency of EEG signals.

The illustration in Fig. 1 shows the epileptic seizure stages, giving a visual picture of the chronological evolution and characteristics of each stage. To identify epileptic seizures, numerous machine learning techniques have been created employing statistical, temporal, frequency, time-frequency domain, and nonlinear factors. In traditional machine learning techniques, features and classifiers are chosen through a process of trial and error. To create a precise model, one needs a solid understanding of data mining and signal processing methods. For little amounts of data, these models work effectively. Machine learning approaches may not work well in the modern era due to the increased availability of data. In order to do this, cutting-edge Deep Learning (DL) algorithms have been used. Unlike traditional machine learning methods, DL models need a lot of data when training. This is due to the fact that these models include numerous feature spaces and encounter the overfitting issue in the absence of data. Deep learning models such as convolutional neural networks (CNNs), recurrent neural networks (RNNs), deep belief networks (DBNs), autoencoders (AEs), CNN-RNNs, and CNN-AEs have been extensively studied to identify epilepsy since 2016. As new effective models are put forth, there are an increasing number of studies in this domain using deep learning (Shoeibi et al.).

A new cross-domain topic of graph-based deep learning has emerged as a result of the adaption of deep learning from images to graphs. This field aims to learn end-to-end informative representations of graphs. Graph networks are part of an emerging field that has had a significant impact on numerous technological fields. Many pieces of information coming from fields like chemistry, biology, genetics, and medicine are more suited for complicated data structures than vector-based representations. Since graphs naturally represent relationships between entities, they could be a particularly helpful encoding method for relational data between variables in these applications. The generalization of graph neural networks (GNN) into non-structural and structural contexts has been a focus of research. The theory of signal processing on graphs has been expanded by graph convolutional networks (GCNs), allowing the representation learning capability of CNNs to be used for irregular graph data. Convolution is made generic to non-Euclidean graph data via graph convolutional networks (Ahmedt-Aristizabal et al., 2021). By combining the properties of a given vertex with those of its neighbors, the graph convolutional operation seeks to provide representations for vertices. The discriminative power of CNN features is substantially increased by the relationship-aware representations produced by GCNs, and the improved model interpretability can assist doctors in identifying, for instance, the regions of the brain that are most active during a specific task. As a result of recent developments in deep learning, it is now possible to identify morphological, textural, and temporal representations of the brain from images and signals using only the data. This has improved the possibility of neural disease analysis. Due to their success in modeling unstructured and structured relational data, including brain signals in the identification and segmentation of neural disorders such as epileptic seizures, Alzheimer's, Dementia, Parkinson's disease, etc., GNNs have experienced a rise in the application.

In comparison to other deep learning networks, DenseNet is more efficient in terms of compute and memory. In order to improve accuracy, DenseNet is a good option for predicting epileptic seizures. Deeper CNN offers improved accuracy, since input data is processed through numerous convolutional processes to produce high-level features, according to recent computer vision research. However, if the input data or gradient goes through multiple convolution layers, it can disappear at the top layer. The vanishing gradient problem was resolved using a dense convolutional network (DenseNet). Each layer in DenseNet receives features from all the levels below it to improve feature propagation (Jana et al., 2019).

A time-frequency decomposition technique that combines the advantages of the short-time Fourier transform (STFT) and wavelet transform (WT) is called the Stockwell transform (S-transform). Time-frequency analysis of EEG signals is useful for identifying seizures because of the non-stationarity characteristics of the EEG signal. Numerous time-frequency approaches have been used for EEG signal analysis, including the Short-time Fourier transform (STFT) and wavelet transform (WT). The Stockwell transform (S-transform), which enables multiresolution analysis with minimal computational cost, is thought to be a mixture of STFT and WT. The S-transform has been extensively used in a variety of industries, including medical imaging, power quality monitoring, and heart sound segmentation. The S-transform is used in the current investigation to represent the time-frequency characteristics of the EEG signals (Geng et al., 2020).

In order to solve the aforementioned concerns, in this paper, we present a unique hybrid deep learning model termed LGCN-DenseNet for the identification of epileptic episodes to address those issues. To classify the output, the model includes a linear graph convolutional network (LGCN) with a DenseNet. A feature extracted from the raw EEG signals using the Stockwell transformation serves as the model's input. The LGCN (Navarin et al., Sperduti) component of the model collects information from each node's neighborhood using a linear filter, allowing for a linear computational cost with respect to the number of edges in the graph. This enables the model to scale to extremely big graphs. Linear classifiers, such as the linear Graph Convolution Network (GCN), can prove useful for analyzing EEG data despite its nonlinearity, severe variability, and potential instability. Compared to nonlinear classifiers, linear classifiers are simpler to construct, more computationally efficient, and can still achieve respectable accuracy for some types of data, including EEG signals. Furthermore, linear classifiers can identify linear correlations within the data, even if the data itself is nonlinear. This means that although EEG signals may not be linear, a linear classifier may still be able to detect linear relationships between different signal characteristics or components. The DenseNet (Huang et al. Weinbergera) component, on the other hand, is well-known for its capacity to

extract features from complicated and high-dimensional data, making it ideal for EEG signal processing. This model can benefit from the best features of both architectures by merging them, making them stronger and more expressive. Additionally, a more reliable representation of the data is made possible by the application of Stockwell transformation to extract features from the raw EEG signals. On the CHB-MIT dataset, we test the effectiveness of this model and demonstrate that it outperforms current state-of-the-art approaches for epileptic seizure identification. The suggested model has the potential to increase seizure detection precision, which could ultimately result in more effective epilepsy management and therapy.

The following are the primary contributions of our work.

1. We propose a hybrid deep learning model called LGCN-DenseNet for automatic seizure detection between inter-ictal and preictal with Stockwell transform as preprocessing technique.
2. In order to fully examine the temporal and spatial relationship between multiple EEG channels, we design the model from the standpoint of graph theory and integrate the properties of LGCN and DenseNet.
3. We run numerous tests on the CHB-MIT dataset. The results revealed that the proposed strategy outperforms rival methods, offering researchers and doctors fresh ideas.

This paper is structured as follows. Section 2 discusses earlier research on seizure detection. Section 3 focuses on the suggested seizure detection approach, the preprocessing method, etc. Section 4 gives a brief overview of the dataset used. Section 5 provides the experimental setup with code and module-based discussions, Section 6 forces on result analysis and a comparison with earlier studies, and Section 8 provides this paper's conclusion.

2. Literature review

Seizure prediction has been the subject of continuing study over the past few years. The fundamental tenet of seizure prediction is that the interictal and preictal phases differ from one another. Early seizure prediction studies frequently employed threshold-based approaches () or machine learning methods like Support Vector Machines (SVM) (Park, Luo, Parhi, Netoff), but more recently, deep learning techniques like CNN (Xu, Ren, Chen, Che) have received significant attention. Liang et al. (Liang, Pei, Cai, Wangb) were the first ones to suggest training a deep-learning classifier to recognize seizures in EEG images, like how doctors identify seizures through visual inspection.

When EEG signals are acquired, noise is added, which lowers the signal-to-noise ratio of the EEG signals and makes it difficult to distinguish between interictal and preictal states (Veisi, Pariz, Karimpour). Bandpass filtering has been employed by Zandi et al. (Shahidi Zandi et al., 2013) for noise elimination. Fast Fourier transform (FFT) has been used by Chu et al. (Chu et al., 2017) to preprocess EEG signals in the frequency domain. Khan et al. (Khan et al., 2018) have applied wavelet transform for preprocessing. Other methods of noise removal from EEG signals include surrogate channels (Korff, Brunklaus, Zuberi) with the help of common spatial pattern filtering. There are two approaches to extracting features: manually creating the features or automatically extracting the features using deep learning techniques.

CNN has received the greatest interest in seizure detection studies employing deep learning systems. Because seizure detection studies utilizing CNN typically require data in the form of images as input, the EEG signal is preprocessed into a two-dimensional format. Xu et al. (Xu, Ren, Chen, Che) offer a one-dimensional convolutional neural network-long short-term memory (1D CNN-LSTM) model for automatic seizure recognition using EEG signals. Using the public UCI epileptic seizure recognition data set, the suggested method achieves high recognition accuracies of 99.39% and 82.00% on the binary and five-class epileptic seizure recognition tasks. Truong et al. (Truong et al., 2018) recommended separating the raw EEG signal by a window size of 30 s, extracting spectrum information using the Short-Time Fourier Transform (STFT), and then feeding it into CNN. Using 64 seizures from 13 patients in the CHB-MIT dataset, the experiment achieved a sensitivity of 81.2% and an FPR of 0.16. To examine the various frequency bands of EEG, Khan et al. (Khan et al., 2018) transform an image into a time-frequency form using Continuous Wavelet Transform (CWT). The authors suggested a method for forecasting seizures that use modified data as input to CNN to learn the difference between interictal and preictal phases. The same dataset was used as before, and after testing 18 seizures from 15 patients, the average FPR was 0.142, with three seizures being unpredictable. Using preprocessed features including spectral band power, statistical moment, and Hjorth parameters as inputs to a multi-frame 3D CNN model, Ozcan et al. (Ozcan & Erturk, 2019) predict seizures with a sensitivity of 85.71% and FPR of 0.096 in the CHB-MIT dataset. In this paper similar work to ours, Ryu et al. (Ryu, Joea) develops a unique hybrid deep learning model that incorporates a Dense Convolutional Network (DenseNet) with Long Short-Term Memory (LSTM). The proposed method first transforms the EEG data into the time-frequency domain using Discrete Wavelet Transform (DWT) for use as model input. The experiment is carried out utilizing the CHB-MIT scalp EEG dataset for each preictal length of 5, 10, and 15 min to evaluate the performance of the proposed technique. When the preictal time was 5 min, we got an F1-score of 0.923 and a sensitivity of 92.92%, with a specificity of 93.65%. The false positive rate was 0.063 per hour, and the detection accuracy was 93.28%. Zeng et al. (Zeng et al., 2021) developed a novel GRP-DNet classification system to identify epileptiform EEG signals. The system takes a single-channel, long-term EEG signal and splits it into non-overlapping short segments using an FNSW. Then, the short segments are converted into GRPs and fed into a DenseNet. The final decision is made using a majority voting strategy. Zhou et al. (Geng et al., 2020) used Stockwell Transformation and bidirectional long short-term memory (BiLSTM). Raw EEG segments are first subjected to the S-transform, and the resulting matrix is organized into time-frequency blocks and sent into the BiLSTM for feature selection and classification. Then postprocessing, which comprises the moving average filter, threshold judgment, multichannel fusion, and collar approach, is used to enhance detection performance. The experiment achieves a sensitivity of 98.09% and a specificity of 98.69%, according to segment-based assessment results. A sensitivity of 96.3% and a false detection rate of 0.24/h are produced for the event-based evaluation.

Other neural network models, such as graph neural networks (GNNs), have been proposed for extracting deep spatial information on seizure detection tasks. Lian et al. (Lian et al.) have applied joint graph structure and representation learning network (JGRN) to classify between preictal and interictal.

3. Proposed method

3.1. System model

System modeling is the process of creating abstract representations of a system. Through this process, various models are created, each of which offers a distinctive perspective on the system under study. This section breaks down the comprehensive system model into three parts: The Method, Data Preparation, and Preprocessing (see Fig. 1).

3.1.1. Method

Fig. 2 depicts the key points of the proposed approach. The raw EEG data is first divided into samples. The adjacency matrix produced by applying the Stockwell transformation and the graph structure data representing the connection between the signal data information and channels is then incorporated into the LGCN model. The retrieved features are then fed into the algorithm's DenseNet section, and the classification is completed by the sigmoid function. As a result, the proposed model trains the difference between interictal and preictal states.

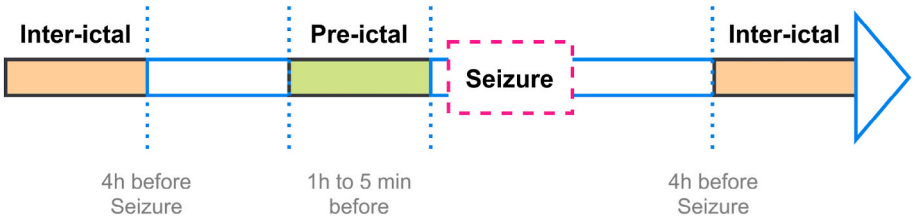

Fig. 1. Stages of epileptic seizure.

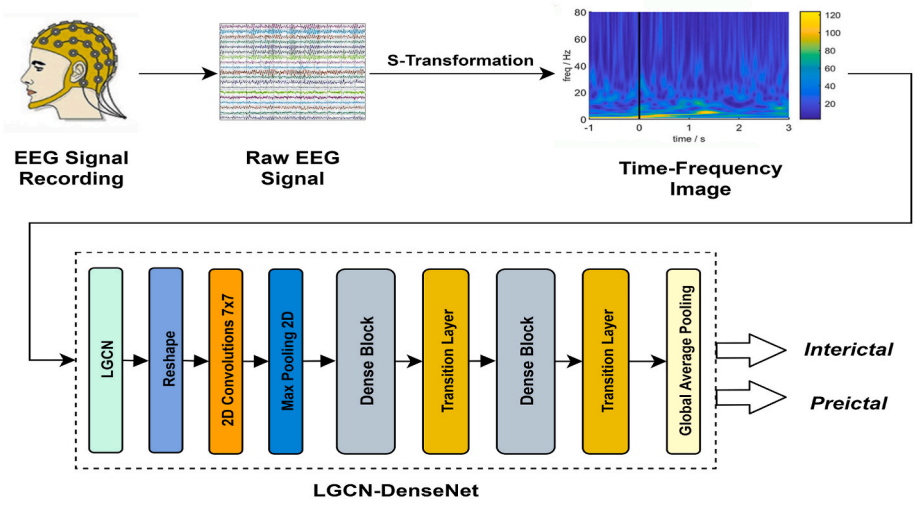

Fig. 2. The system model of proposed method.

3.1.2. Data Preparation

To ensure an adequate amount of experimental data, continuous data is assumed to span a lengthy period. During the study of other state-of-the-arts methods for setup. U sing trial and error methods, we have set the parameters to get the best possible outcome based on our hardware specification. For instance, long-term EEG data is segmented into multiple smaller fragments. This is done by dividing the data into several time periods using a sliding window technique with a 1-s period and a 0.5 overlap rate. As an example, a 60-s EEG signal with a sampling frequency of 1 Hz would be represented as a 60-s vector, divided into 100 epochs. Once the data is segmented, a suggested method linearly examines and categorizes the labels of different periods. During the study of other state of the art methods about similar.

Preictal time usually limits between 5 min and 1 hour before seizure happened (Chen et al., 2021; Zhang et al., 2020). For detecting preictal states properly, we have set the time 5,10 and 15 min based on trial and error methods similar to (Ryu, Joea; Lian et al.) for the best possible outcomes.

To solve the issue of data imbalance, a data augmentation strategy is applied to the training set to reduce overfitting (Salamon & Bello, 2017). We choose one or two seizure episodes at random for each patient and count the number of normal EEG recordings that are 5 times as large as the seizure data in the training set. The seizure data is then augmented in such a way that each seizure episode is resampled five times.

3.1.3. Preprocessing

The suggested technique's overall system model is shown in Fig. 2. The first step involves preprocessing the EEG signal before inputting it into the deep learning model. The raw EEG data is divided into channels, then into window sizes, and transformed into a time-frequency type 2D image using the S-Transform. The preprocessed data is then used as input data for the Linear Graph Convolution Network (LGCN), and the resulting feature map is used as input data for the DenseNet.

3.2. Stockwell Transformation

The Stockwell Transformation or S-transform was proposed by Stockwell et al. (Stockwell et al., 1996) by combining the merits of STFT (Short Time Fourier Transform) and WT (Wavelet Transform), which has gained considerable attention in several fields of science and engineering including geophysics, optics, biomedical imaging, oceanology, bioinformatics, and signal processing. It is remarkable in that it gives frequency-dependent resolution while remaining directly related to the Fourier spectrum. Furthermore, the classical S-transform can be seen of as a phase-corrected WT, offering more precise information on a signal's local features in a time-frequency analysis. This makes the S-transform more resistant to non-stationary signals and, in some cases, provides better time-frequency resolution.

In Fig. 3, The EEG signal is initially divided into separate channels and segmented with a window size of 1 s. Subsequently, the Stockwell transform is individually applied to each channel to obtain a time-frequency representation of the signal. In addition, the short-time Fourier transform (STFT) is applied, resulting in a complex-valued matrix that describes the signal's frequency content at various time points. This process enables the extraction of multi-channel data by independently applying the transformation to each channel. Take the natural logarithm of the result of the square of the STFT magnitude. This is known as the modulation step, and it makes the S-transform more sensitive to changes in the frequency content of the signal over time. Now when we apply the inverse STFT to modulation step output, it will finally give us a two-dimensional image of the signal's frequency content (see Fig. 4).

Let $\psi \varepsilon L^1(\mathbb{R}) \cap L^2(\mathbb{R})$ be such that $\int_{-\infty}^{\infty} \psi(t)dt = 1$, the S-transform of a signal $x(t)$ in $L^2(\mathbb{R})$ with respect to the window function $\psi(t)$ is defined by,

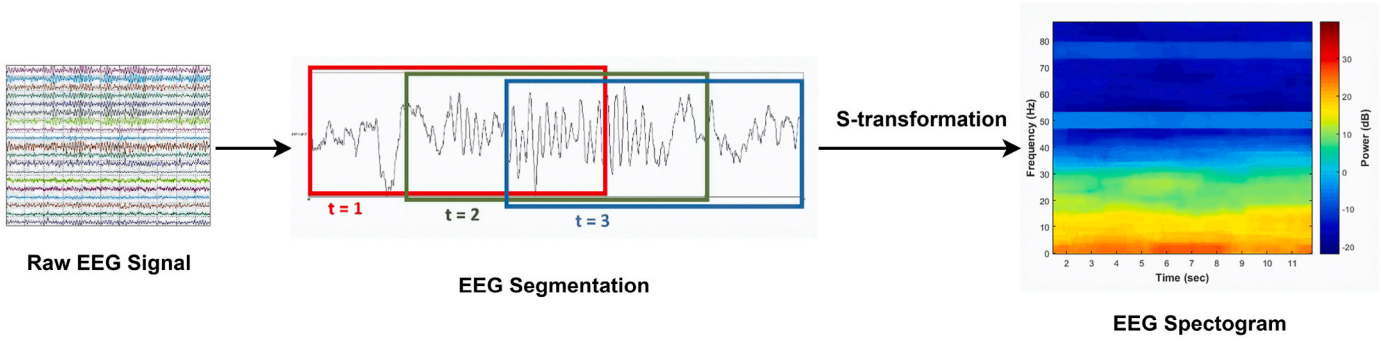

Fig. 3. Steps of Converting Raw EEG signal into frequency image using Stockwell Transformation.

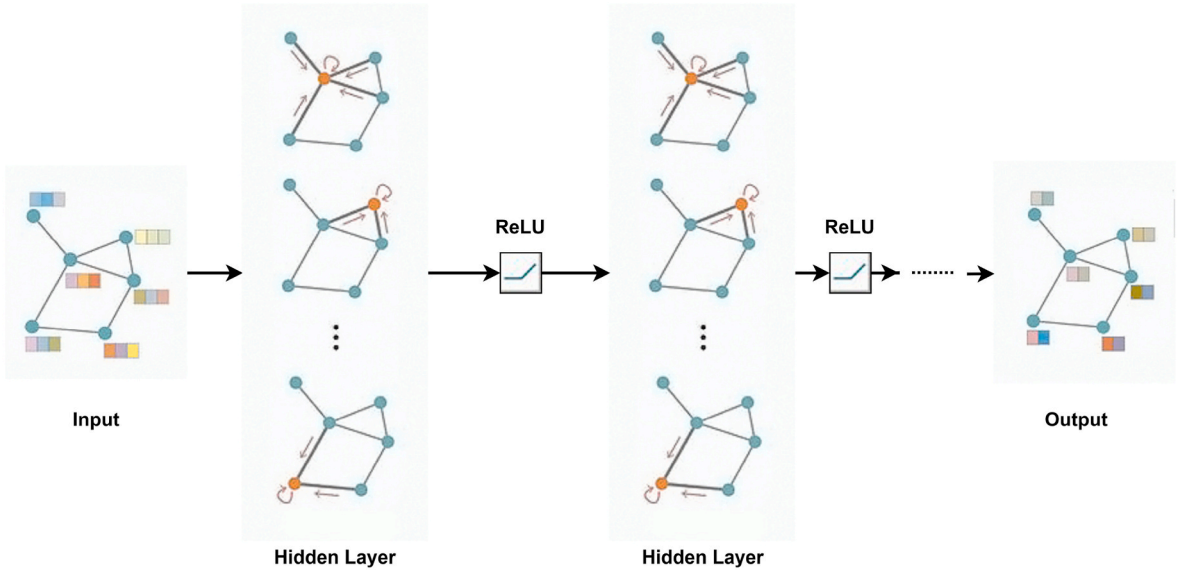

Fig. 4. Linear graph convolutional network for seizure detection.

$$ST_x(t,f) = |f| \int_{-\infty}^{\infty} x(\tau)\overline{\psi(|f|(\tau - t))}e^{-j2\pi\tau f} d\tau, t\varepsilon\mathbb{R}, \tag{1}$$

Where, $f \in \mathbb{R}/\{0\}$. At zero frequency $f = 0$, the S-transform is equal to the average of the signal *i.e.*,

$$ST_x(t,0) = \int_{-\infty}^{\infty} x(\tau)d\tau \tag{2}$$

The S-transform can also be defined in the frequency domain, *i.e.*,

$$ST_x(t,f) = \int_{-\infty}^{\infty} X(\alpha + f)\overline{\Psi\left(\frac{\alpha}{|f|}\right)}e^{j2\pi\alpha t} d\alpha, \tag{3}$$

Where, $t \in \mathbb{R}$ and $f \in \mathbb{R}/\{0\}$. $\Psi(f)$ is the Fourier spectrum of the signal x and the window function ψ, respectively.

Each segment's S-transform yields a 1024 × 128 time-frequency matrix, where 128 represents frequency from 1 to 128 Hz and 1024 represents time points. Seizure activity often occurs at frequencies ranging from 3 to 30 Hz. As a result, the proposed S-transform spectrogram has a frequency range of 4–32 Hz. Furthermore, to reduce our system's calculation complexity, the time-frequency matrix is partitioned into 64 blocks in the time axis and 14 blocks in the frequency axis. By aggregating the power in each block, 896 blocks are formed. Finally, following the S-transform in this study, a 14 × 64 matrix is created, which will be used as the input of LGCN.

3.3. Linear Graph Convolution Network (LGCN)

It is clear that there are differences in the correlation between the various channels. The association between EEG waves recorded from nearby electrodes is stronger. As a result, the spatial information that the EEG signals provide will be crucial in the seizure detection process. Y. Zhao et al. provide a seizure detection model based on LGCN that is motivated by this idea (Zhao et al., 2021).

A graph is used to model distinct EEG signals from different channels. The raw EEG data is represented by the graph's nodes, which stand for the feature vector of EEG signals. Pearson correlation analysis is used to create the adjacency matrix, which is then binarized using a manually chosen threshold. The obtained adjacency matrix has elements that are either 0 or 1. The LCCN discussed here consists of two layers. Each node aggregates the first-order node characteristics in the first layer, updating its own node embeddings. Each node is embedded in a weighted sum average feature that keeps its own properties and superimposes all first-order neighbour data in the second layer. Each node continues to collect its own first-order node features in the same manner on the basis of superimposing information. The seizure detection is then made possible at the ReLU layer by combining the properties of two LGCN layers into one fully connected layer. The whole process of LGCN for seizure detection are shown in Figure 4. The convolution rules of LGCN are as follows:

$$H^{(l+1)} = \sigma\left(\widetilde{D}^{\frac{-1}{2}}\widetilde{A}\widetilde{D}^{\frac{-1}{2}}H^{(l)}W^{(l)}\right) \tag{4}$$

Where, $\widetilde{A} = A + I_N$ represents the graph's adjacency matrix, I_N represents the identity matrix, and $\widetilde{D}_{ii} = \sum_j \widetilde{A}_{ij}$ is the degree matrix, and $W^{(l)}$ is a trainable weight matrix. Furthermore, $\sigma(\bullet)$ denotes an activation function, and the activation function of Relu is used to add a nonlinear element. $H^{(l)} \in R^{N\times D}$ denotes the activation matrix of the L layer. $H^{(0)} = x$. This experiment's initial inputs are node feature x and the adjacency matrix A.

3.3.1. Graph Convolution Network (GCN)

The proposed LGCN model investigated the relationship between the electrode pairs in the International 10–20 system in terms of physical position. Authors define raw EEG signals as x and the convolution kernel g_θ = diag(θ) in the fourier domain with parameters θ∈RˆN. The spectral convolution on graphs x and gθ is calculated as follows:

The proposed LGCN model investigated the relationship between the electrode pairs in the International 10–20 system in terms of physical position. Authors define raw EEG signals as x and the convolution kernel $g_\theta = diag(\theta)$ in the Fourier domain with parameters $\theta \in R^N$. The spectral convolution on graphs x and g_θ is calculated as follows:

$$g_\theta \star x = U g_\theta U^T x \tag{5}$$

Where, U is the eigenvector matrix obtained by the symmetric normalized Laplacian operator.

$$L = I_N - D^{-1/2} A D^{-1/2} = U \Lambda U^T \tag{6}$$

Where, Λ and $U^T x$ denote the eigenvalue matrix and the Fourier transform of x Calculating U is expensive. As a result, the k-order Chebyshev polynomials are used to approximate.

$$g_{\theta'}(\Lambda) \approx \sum_{k=0}^{K} \theta'_k T_k(\widetilde{\Lambda}) \tag{7}$$

Where, $\widetilde{\Lambda} = 2\Lambda/\lambda_{max} - I_N$ and $\theta' \in R^K$ denote the Chebyshev coefficient vector. $T_k(x) = 2xT_{k-1}(x) - T_{k-2}(x)$, where $T_0(x) = 1, T_1(x) = x$ is the Chebyshev polynomial. With these estimates,

$$g_{\theta'} \star x \approx \sum_{k=0}^{K} \theta'_k T_k(\widetilde{L}) x \tag{8}$$

Where, $\widetilde{L} = \frac{2}{\lambda_{max}} L - I_N$ and depicts the Chebyshev kth order approximation, which reduces model parameters and calculation complexity.

3.3.1.1. Chebyshev's linear model. When k = 1, above mentioned equation can be simplified as,

$$g_{\theta'} \star x \approx \theta'_0 x + \theta'_1 (L - I_N) x = \theta'_0 x - \theta'_1 D^{-\frac{1}{2}} A D^{-\frac{1}{2}} x \tag{9}$$

Let, $\theta = \theta'_0 - \theta'_1$, and we get the following approximation:

$$g_\theta \star x \approx \theta \left(I_N + D^{-\frac{1}{2}} A D^{-\frac{1}{2}} \right) x \tag{10}$$

However, using the operation directly in a deep neural network model will result in gradient explosion or disappearance. As a result, the following normalization technique is introduced:

$$I_N + D^{-\frac{1}{2}} A D^{-\frac{1}{2}} \rightarrow \widetilde{D}^{-\frac{1}{2}} \widetilde{A} \widetilde{D}^{-\frac{1}{2}} \tag{11}$$

Where, $\widetilde{A} = A + I_N$ and $\widetilde{D}_{ii} = \sum_j \widetilde{A}_{ij}$. It is possible to obtain the layer-wise linear form GCN model

$$H^{(l+1)} = f(H^l, A) = \sigma\left(\widetilde{D}^{-\frac{1}{2}} \widetilde{A} \widetilde{D}^{-\frac{1}{2}} H^{(l)} W^{(l)} \right) \tag{12}$$

3.4. DenseNet

DenseNet is a type of convolutional neural network (CNN) that is designed to be efficient and effective for image recognition tasks. It was developed at the Chinese University of Hong Kong in 2016 (Huang et al., Weinbergerb). DenseNet's key innovation is "dense connections," with each layer receiving input from all previous layers. This enables more efficient learning and outperforms other CNNs in image classification. Advantages include reduced computation and parameters and addressing the issue of vanishing gradients.

As illustrated in Fig. 5, dense connectivity is a means of continuously connecting the previous layer's feature map with the input of the subsequent layer to reinforce information flow between levels.

DenseNet has Dense Blocks and Transition Layers. Dense Blocks have bottleneck layers and growth rates, and multiple layers are connected using channel-wise concatenation. This can increase network parameters and decrease computation efficiency.

To overcome this oversized parameter problem, the authors of DenseNet find a solution that is using the growth rate (=k) as a hyperparameter, and then apply the Batch Normalization (BN) - > Rectified Linear Unit (ReLU) - > Conv (1 × 1) - > Batch Normalization (BN) - > ReLU - > Conv (3 × 3) nonlinear transformation to the DenseNet structure. The bottleneck layer is depicted in Fig. 6. Furthermore, as previously stated, it is utilized to reduce the amount of input feature maps and enhance calculation efficiency.

As shown in Fig. 7, the transition layer is responsible for lowering the width and height of feature maps as well as the number of feature maps. It is linked behind the dense block and comprises of BN - > ReLU - > Conv (1 × 1) - > Avg pool (2 × 2). The compression factor, which has a value between 0 and 1, is now used to specify how much the feature map should be shrunk. If this value is set to 1, the number of feature maps remains constant. Furthermore, DenseNet applied the composite function consisting of the order of BN - > ReLU - > Conv to the layer (see Fig. 8).

3.5. Hybrid model

This work presents a hybrid model that combines LGCN with DenseNet. The suggested model uses the LGCN algorithm to build its first half. It uses the feature map from this section as DenseNet input data to represent the spatial and structural information on the feature, and then propose a hybrid model that classifies using the sigmoid function. In particular, the input data are picture data that have been converted by applying S- transform to the raw EEG signal and consist of frequency, time, and channel. Then images are transformed into a graph representation so that it can be used as an input graph. After processing through LGCN, the output of the feature is used as the input of DenseNet. The Conv layer creates an output feature map from the input data that is twice as fast as the growth rate. Following that, all dense blocks have the same number of layers, and Conv (3 × 3) in them does 1-pixel zero-padding to keep the size of the feature map constant. The transition layer is used after the dense block. Conv (1 × 1) and average pooling are used to minimize the size of the feature map in transition layers. Lastly, the features generated through DenseNet are categorized as interictal or preictal states using the Sigmoid function.

4. Dataset

Dataset is taken from Boston Children's Hospital (CHB) and the Massachusetts Institute of Technology (MIT), which is publicly available in PhysioNet.org (Shoeb & Guttag, 2010), and contains scalp electroencephalogram (sEEG) data from 23 pediatric subjects.

Scalp EEG waves were recorded with 23 electrodes at a sampling rate of 256 Hz. Fixed 23-electrode setups are employed in 15 tests, with some electrode configuration variations in the remaining measurements. The recordings are organized into 24 cases, with most of the 24 cases

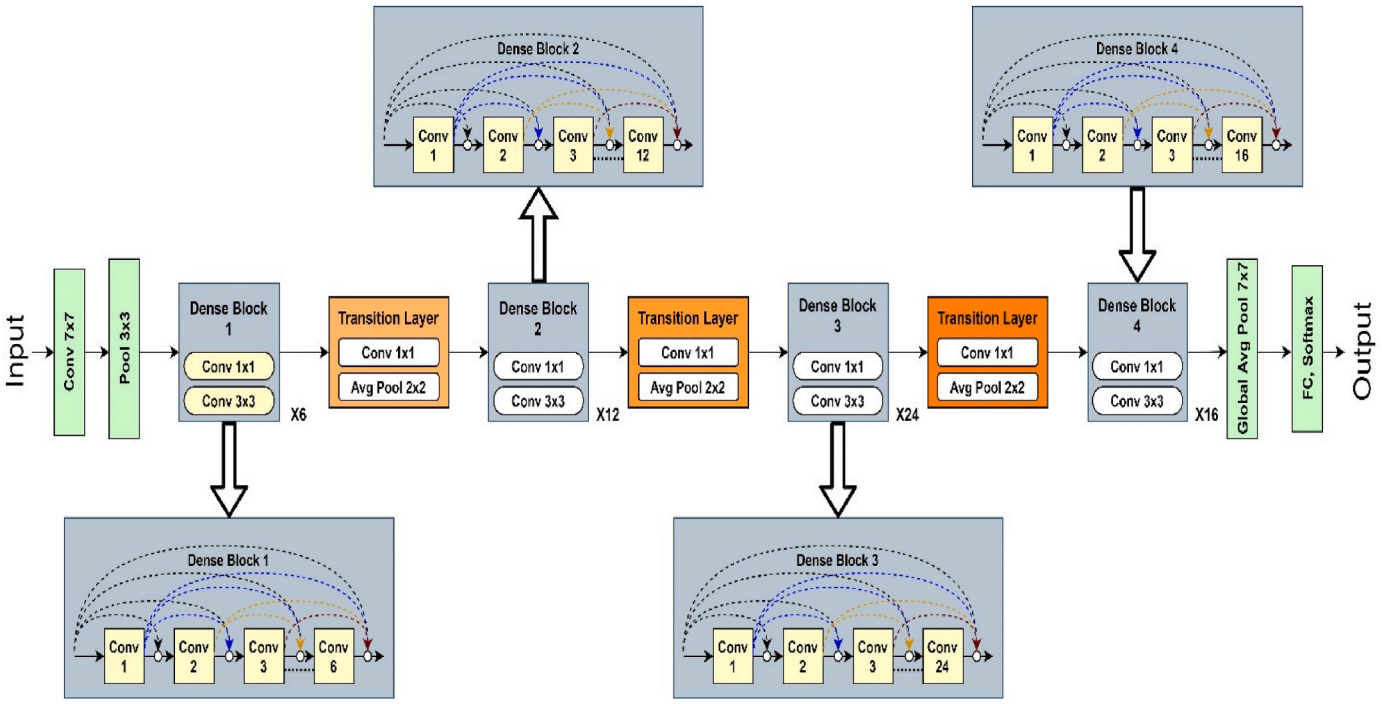

Fig. 5. DenseNet architecture.

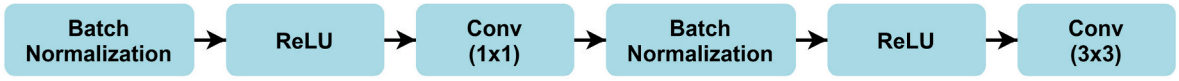

Fig. 6. Dense block.

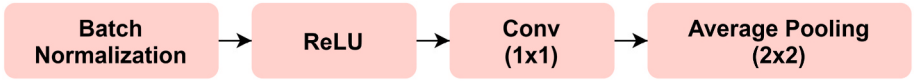

Fig. 7. Transition block.

segmenting the EEG signals into 1-h epochs, but epochs lasting 2–4 h can also be found. The overall length of the accessible EEG recordings is around 877.39 h. In all, 877.39 h of EEG data were used in this study, with 2.50 h used for training and 874.89 h used for assessing performance. According to the database's annotation files, most of the 24 cases have frequent changes in the EEG signal recording montage, with channels being added or removed from one epoch to the next during the recording process. There are 18 channels in total that are consistent across all 24 cases, including: {"FP1–F7", "F7-T7", "T7-P7", "P7–O1", "FP1–F3", "F3–C3", "C3–P3", "P3–O1", "FP2–F4", "F4–C4", "C4–P4", "P4–O2", "FP2–F8", "F8-T8", "T8-P8", "P8–O2", "FZ-CZ" and "CZ-PZ"}. The CHB-MIT dataset lacks preictal and interictal labels, however they can be retrieved using seizure timings from each patient's meta-data file. This is applicable in all circumstances except Case 24, where the file's start and end times are not stated. To identify interictal states, a specific distance from the ictal phase must be maintained, but this may vary among patients. Patients with small distances use interictal periods that are far from the ictal phase, while those with sufficient distance use periods further away. We assume the pre-ictal state lasts at least an hour based, and the interictal state occurs 4 h before or after the seizure. The model excludes the 5-min interval before the seizure onset, and prompt intervention is necessary for seizure control.

5. Experiment

5.1. Procedure

Since 1 s of EEG signal for 18 channels is considered, the input image's dimensions are $192 \times 256 \times 18$. The proposed DenseNet is made up of 5 dense blocks, each of which comprises 4 consecutive convolutional layers (dense layers). In the dense block, a growth rate of 32 is applied. Each dense block increases dense layers by 12, transition layers use 1×1 conv and 2×2 pooling. A dropout operation (not displayed in the table) with a value of 0.25 is also included after each convolutional layer to prevent the network from over-fitting. Dense block, global average pooling, sigmoid classifier classify pre-ictal/inter-ictal states. The detailed configurations of DenseNet are shown in Table 2.

The k-fold cross-validation approach is used in the experiment. The data is divided into k folds for K-fold cross-validation, which trains with k-1 and tests with the remaining k folds. The model's verification result is the average of the result values acquired by repeating this method k times.

Many characteristics, such as the number of channels, interictal period, preictal period, and record continuity, vary among all subjects. And for that a total of 22 electrode channels, we used 18 channels. The distance from ictal phase determines interictal period, with variations for each patient. Two cases: close distance uses far interictal, while sufficient distance uses beyond a specific distance. Pre-ictal state lasts an

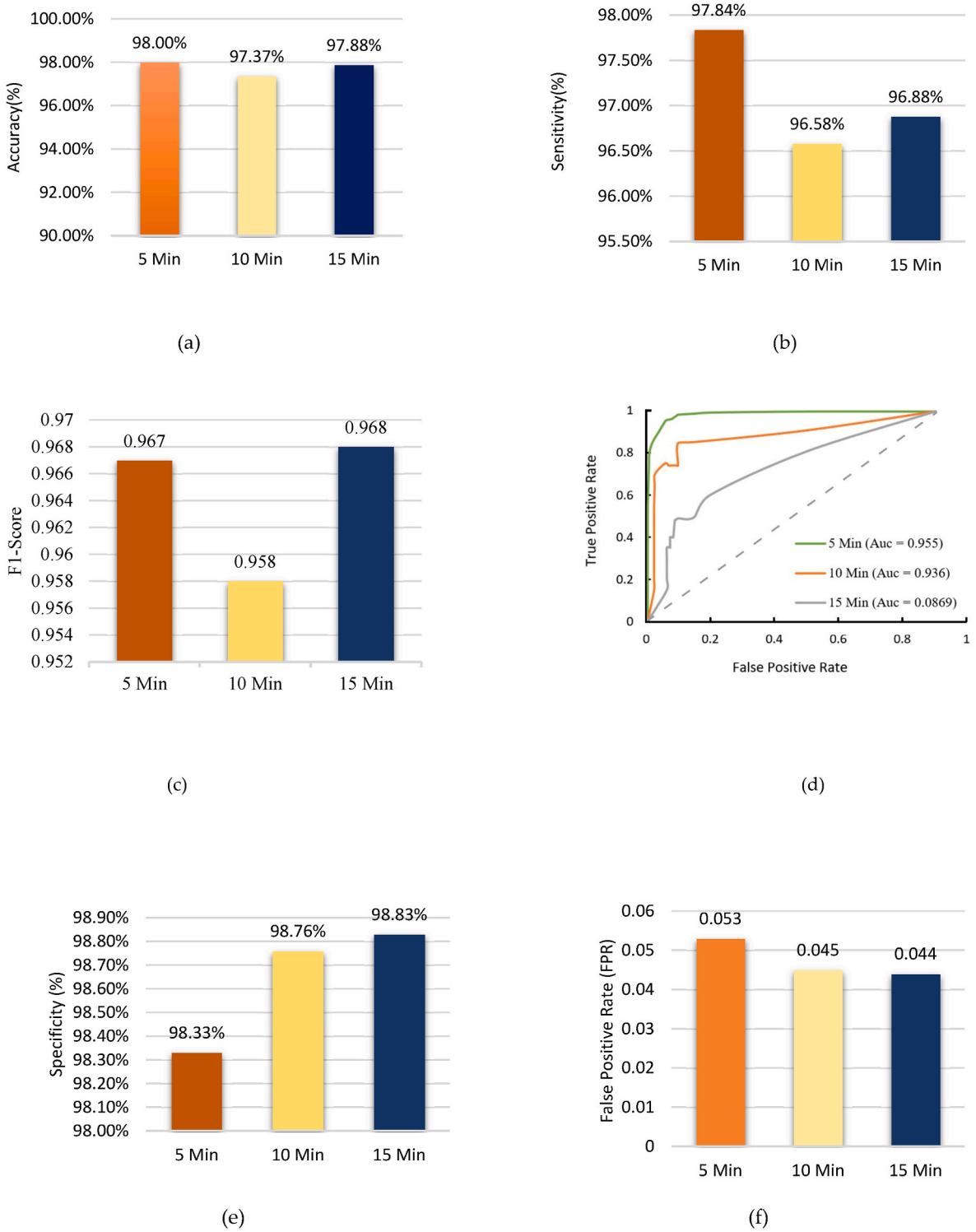

Fig. 8. Accuracy (a), sensitivity (b), specificity (c), false positive rate (d), F1-score (e), and ROC curve (f) averaged over preictal lengths of 5, 10, and 15 min.

Table 1
Band frequency of EEG signals (Saminu et al., 2021).

Band	Frequency (Hz)
Delta	1–4 Hz
Theta	4–7.5 Hz
Alpha	7.5–13 Hz
Lower Beta	13–16 Hz
Higher Beta	16–30 Hz
Gamma	30–40 Hz

hour, and interictal occurs 4 h before/after seizure. For seizure detection, the 5-min interval before seizure is excluded. If a seizure is predicted, 5 min are needed for immediate treatment.

5.2. Ablation tests

Using the LGCN model, the DenseNet model, and the suggested LGCN-DenseNet model, we conduct experimental comparisons to validate the combined contribution of LGCN and DenseNet in our model.

Table 2
The Configuration of DenseNet.

Layer	Operations	Output
Convolution Layer	Convolution using 24 filters of 7 × 7 with stride 2	96 × 128 × 24
Pooling Layer	Sub-sampling using max pooling of 3 × 3 filter with stride 2	48 × 64 × 24
Dense Block	4 times convolution using 3 × 3 filter	48 × 64 × 72
Transition Layer	Convolution using 1 × 1 filter, then average-pooling using 2 × 2 filter with stride 2	24 × 32 × 72
Dense Block	4 times convolution using 3 × 3 filter	24 × 32 × 120
Transition Layer	Convolution using 1 × 1 filter, then average-pooling using 2 × 2 with stride 2	12 × 16 × 120
Dense Block	4 times 3 × 3 convolution	12 × 16 × 168
Transition Layer	Convolution with 1 × 1 filter, then average-pooling using 2 × 2 filter with stride 2	6 × 8 × 168
Dense Block	4 times convolution using 3 × 3 filter	6 × 8 × 216
Transition Layer	Convolution using 1 × 1 filter, then average-pooling using 2 × 2 filter with stride 2	3 × 4 × 216
Dense Block	4 times convolution using 3 × 3 filter	3 × 4 × 264
Classification Layer	Global average pooling	1 × 1 × 264
	2 output classes fully connected network with Sigmoid activation	2

The same model parameters are used throughout all experiments to guarantee consistency and reliability. Table 7, displays the outcomes. Table 3, shows that the suggested LGCN-DenseNet model outperforms the LGCN and DenseNet models using the same EEG characteristics in three different metrics, demonstrating the robustness and effectiveness of EEG signal processing. Incorporating the best features of both algorithms into a single model greatly enhances its capacity for learning.

6. Result analysis

6.1. Productive setup

Here we will discuss the setup of our workstations, the hyperparameters of our model of LGCN-Densenet, the methods we used to conduct our experiments, and the metrics we used to evaluate our results Table 4, shows that a 32 GB RAM and an Intel Core i7-12700 CPU were utilized. The suggested model was trained on a computer with a GPU (graphics processing unit) from Nvidia's GeForce RTX 3060 Ti series. The software stack being tested consists of Python 3.9, Keras 2.3.1, and Tensorflow 2.6.0.

As a hyperparameter of, the growth rate was set to 32 and the compression factor was set to 0.5, as shown in Table 5. Additionally, as indicated the optimizer that will be utilized is Adam, and the activation function will be Leaky ReLU. The learning rate will be 0.001, and it will be set to that value.

6.2. Evaluation metrics

The model's effectiveness is measured in this study using five statistical measures: sensitivity, specificity, accuracy, F1-score, and area under the receiver operating characteristic curve (AUC). The formula for

Table 3
Individual tests on each model.

Method	Accuracy	Sensitivity	Specificity
LGCN	95.29%	93.62%	94.44%
DenseNet	92.45%	85.65%	91.19%
LGCN-DenseNet	98.00%	97.84%	98.33%

Table 4
Hardware setup.

Software or Hardware	Specification
CPU	Intel Core i7-12700
GPU	GeForce RTX 3060 Ti
RAM	DDR4 32 GB
Python	3.9
Tensorflow	2.6.0
Keras	2.3.1

Table 5
Hyperparameter setup.

Hyperparameters	Values
Growth rate	32
Compression factor	0.5
Activation function	Leaky ReLU
Optimizer	Adam
Learning rate	0.001

calculating sensitivity is as follows:

$$Sensitivity = \frac{TP}{TP + FN} \tag{13}$$

In this context, TP refers to the total number of correctly detected epileptic seizure pieces. FN is an abbreviation for "false negatives," which stands for the total number of misidentified seizure items. In all positive cases, sensitivity gives a precise representation of the proportion. The recall number is identical to that one.

Accurately determining a target's specificity requires the following:

$$Specificity = \frac{TN}{TN + FP} \tag{14}$$

where TN stands for "true negatives," which refers to the total number of correctly detected non-epileptic components. The acronym FP, which stands for "false positives," denotes the number of improperly detected seizure fragments. Precision is the frequency with which erroneous positives are ruled out. We use the following formula to determine accuracy:

$$Accuracy = \frac{TP + TN}{TP + TN + FP + FP} \tag{15}$$

This indicates the proportion of valid predictions made throughout the whole set of samples. F1-score and precision may be computed as follows:

$$F1 - Score = \frac{2 * precision * recall}{precision + recall} \tag{16}$$

$$Precision = \frac{TP}{TP + FP} \tag{17}$$

The F1-score is a measurement of how accurate a binary classification model is by taking the harmonic mean of the precision and recall values. Precision and recall could be measured in their whole via the use of this approach since both aspects are also included. Precision may be described as the proportion of the actual number of positive samples to the total number of samples that were projected to be positive. The area under the ROC curve, often known as the AUC, is a model assessment indicator that is used for classification tasks. The integral value of the ROC curve is the approach that is used to calculate the AUC.

7. Discussion

Using the Stockwell transformation, time-frequency characteristics may be extracted, which is essential for capturing the dynamic changes in EEG data that take place during seizures. There is no universally

accepted duration for the preictal state. Based on the other studies available in the literature (Chen et al., 2021; Salamon & Bello, 2017; Li et al., 2022), in this study we choose a preictal duration of at least 5, 10 or 15 min before seizure, as such period is supported in (Ryu, Joea;). Fig. 8 depicts the average Acc, Sen, Spec, FPR, and F1-scores for preictal lengths of 5, 10, and 15 minutes. According to the experimental data, the model trained under the premise that a preictal length of 5 minutes assures greater sensitivity than preictal lengths of 10 and 15 minutes. In comparison to typical time-domain or frequency-domain features, this can offer a more robust and useful feature representation. LGCN efficiently captures structural information in EEG signals. Given that seizures frequently present as aberrant patterns in the underlying brain activity, this can be especially helpful in treating seizures. Combining LGCN and DenseNet creates an effective model that recognizes intricate patterns in data with many dimensions. The model can better detect seizures, being more resilient to noise, missing data, and outliers frequently present in EEG signals. Table 6 shows the accuracy results of our model.

Table 6 presents the mean accuracy, sensitivity, specificity, false positive rate, and F1-score for each patient, categorized by the chosen preictal length. The model assuming a preictal length of 5 min demonstrates the highest average sensitivity. However, it is worth noting that for patient 7, the sensitivity is lower for the 5-min model compared to the 10- and 15-min models. This indicates that the preictal characteristics did not manifest prominently during the initial 0–5 min period for patient 4, but became more apparent after 5 min. Conversely, for patient 23, the sensitivity of the trained model was relatively lower for the 10- and 15-min models compared to the 5-min model. This suggests that the preictal features were more distinct during the 0–5 min period for patient 24. Overall, the model assuming a preictal length of 5 min achieved the best average performance. However, the model assuming a preictal length of 15 min demonstrated a balanced outcome without significantly compromising the results for each patient.

This proposed method was compared to already-in-use algorithms in order to unbiasedly assess its efficiency (Khan et al., 2018; Truong et al., 2018; Ozcan & Erturk, 2019;). A method of transforming EEG signals into picture data by STFT and categorizing them through CNN was proposed by the authors of (Khan et al., 2018). In this paper (Truong et al., 2018), employs CWT to convert an EEG signal into picture data, and CNN is used for classification. The authors of (Ozcan & Erturk, 2019) predicted seizures by feeding Hjorth parameters as input to 3D-CNN. In (Zhao et al., 2021), EEG signal is transformed into image data using DWT and uses customized hybrid model (DenseNet-LSTM) to classify. As shown in Table 7, this proposed method outperforms the existing method in terms of performance.

8. Conclusion

This work's experimental results and comparisons with previous studies shows that this proposed method is efficient and reliable. This method achieved 98% detection accuracy, 97.84% sensitivity, 98.60% specificity, 0.069 hourly FPR, and 0.967 F^1-score. This suggests that it has the potential to be used as a seizure detection tool to effectively mitigate the risk of epilepsy patients. LGCN works very well with other deep learning architectures such as CNNs, RNNs and LSTMs to produce more potent models, which are especially helpful when dealing with time series data and sequential data. The DenseNet technique, which improves the existing CNN problem addressed in this study, improves information flow throughout the network and increases computational efficiency. DenseNets are well-known for their capacity to collect complicated features in images as well as perform well on image classification tasks. The proposed method has to be thoroughly evaluated with more EEG data because the majority of the CHB-MIT dataset's patients are children. However, the results of this work and comparisons with other research demonstrate the effectiveness and dependability of the suggested approach. This demonstrates the possibility of using a seizure detection technology to successfully lessen the harm posed by epilepsy sufferers. In future work, we are planning to test our proposed model on additional datasets to further evaluate its performance and generalizability. We are also trying to improve our preictal detection system so that it can detect the exact start point of the preictal period.

Funding

"This research received no external funding".

Table 6
Results of seizure detection based on preictal length in 24 patients from the CHB-MIT scalp EEG dataset.

Patients	Preictal Length: 5 min					Preictal Length: 10 min					Preictal Length: 15 min				
	Acc. (%)	Sen. (%)	Spec. (%)	FPR	F1–S	Acc. (%)	Sen. (%)	Spec. (%)	FPR	F1–S	Acc. (%)	Sen. (%)	Spec. (%)	FPR	F1–S
01	100	100	100	0	1	100	100	100	0	1	100	99.96	100	0	0.999
02	95.94	97.97	95.91	0.109	0.989	95.89	98.79	98.98	0.01	0.977	97.89	98.86	98.99	0.01	0.897
03	96.82	96.30	97.33	0.024	0.967	96.86	94.49	99.23	0.012	0.908	96.98	94.99	99.26	0	0.909
04	98.26	95.46	96.06	0.062	0.977	98.46	99.80	96.11	0.093	0.98	98.46	99.86	96.09	0.098	0.991
05	98.32	97.82	97.83	0.041	0.946	97.29	96.56	98.02	0.02	0.972	97.29	96.56	98.56	0.02	0.987
06	94.20	98.61	99.78	0.004	0.902	96.60	95.41	97.79	0.052	0.963	96.60	95.79	97.68	0.058	0.961
07	100	100	100	0	1	99.40	98.81	100	0	0.993	99.40	98.88	100	0.015	1
08	100	100	100	0	1	100	100	100	0	1	100	100	100	0	1
09	99.82	99.25	100	0	0.998	98.64	99.28	100	0	0.916	98.94	99.25	100	0	0.999
10	98.52	98.11	98.24	0.13	0.916	97.58	90.45	99.72	0.096	0.913	97.58	90.98	99.72	0.096	0.985
11	100	100	100	0	1	100	100	100	0	1	100	100	100	0	0.995
12	97.07	96.99	99.16	0.008	0.879	95.91	94.39	99.43	0.025	0.953	95.91	94.97	99.43	0.036	0.961
13	98.05	99.41	99.14	0.103	0.922	91.05	88.19	98.90	0.08	0.906	96.95	90.26	98.76	0.008	0.889
14	95.32	97.20	98.03	0.115	0.901	95.19	90.66	98.93	0.012	0.931	97.79	90.66	98.82	0.019	0.974
15	98.43	95.30	96.02	0.118	0.902	98.97	97.12	99.82	0.093	0.94	98.97	97.12	99.75	0.049	0.947
16	99.03	91.20	90.86	0.091	0.778	97.33	91.40	98.27	0.087	0.97	97.33	93.90	98.27	0.087	0.972
17	100	100	100	0	1	99.80	100	99.60	0.004	0.998	99.80	100	99.60	0	1
18	97.03	98.06	99.64	0.003	0.92	95.23	95.72	90.73	0.092	0.936	95.23	95.72	92.06	0.098	0.967
19	100	100	100	0	1	100	100	100	0	1	100	100	100	0	1
20	99.96	100	99.93	0	0.999	99.86	100	99.72	0.002	0.998	99.89	100	99.89	0.004	0.998
21	95.40	98.66	98.99	0.03	0.952	93.36	91.87	99.83	0.051	0.932	93.70	91.89	99.83	0.032	0.994
22	97.31	97.04	96.68	0.3	0.836	91.61	98.43	98.79	0.112	0.928	91.83	98.59	98.79	0.106	0.988
23	96.06	96.01	97.42	0.026	0.966	99.01	99.05	96.97	0.17	0.933	99.65	99.05	96.97	0.180	0.95
24	96.46	94.76	98.96	0.11	0.825	98.93	97.47	99.38	0.076	0.955	98.93	97.76	99.38	0.076	0.878
Mean	**98.00**	**97.84**	**98.33**	**0.053**	**0.967**	**97.37**	**96.58**	**98.76**	**0.045**	**0.958**	**97.88**	**96.88**	**98.83**	**0.044**	**0.968**

Table 7
Comparison (5 minutes of preictal length) of the proposed method with other state of art.

Authors	Year	Classifier	Acc. (%)	Sen. (%)	Spec. (%)	FPR (H)	F1-Score
Khan et al. (2018)	2017	CNN	88.01	87.8	88.33	0.147	0.781
Truong et al. (2018)	2018	CNN	80.58	81.2	80.69	0.16	0.729
Ozcan et al.	2019	3D CNN	86.67	85.71	86.67	0.096	0.862
Ryu S al.	2021	DenseNet-LSTM	93.28	92.92	93.65	0.063	0.923
Proposed Method	**2023**	**LGCN-DenseNet**	**98.00**	**97.84**	**98.33**	**0.053**	**0.967**

9. Institutional review board statement

"Not applicable".

Informed consent statement

"Not applicable."

Data availability statement

All data are available in the manuscript.

Declaration of competing interest

Declare conflicts of interest or state "The authors declare no conflict of interest".

Acknowledgments

This study was supported by the International Research Networks Grant Scheme 2.0 (Grant No. STR-IRNGS-SETCAPRT- 01-10 2022), Sunway University, Malaysia.

Appendix A. Supplementary data

Supplementary data to this article can be found online at https://doi.org/10.1016/j.jrras.2023.100607.

References

Ahmedt-Aristizabal, D., Armin, M. A., Denman, S., Fookes, C., & Petersson, L. (2021). Graph-based deep learning for medical diagnosis and analysis: Past, present and future. In *Sensors, 21*MDPI AG. https://doi.org/10.3390/s21144758, 14.

Boonyakitanont, P., Lek-uthai, A., Chomtho, K., & Songsiri, J. (2019). *A comparison of deep neural networks for seizure detection in EEG signals*. https://doi.org/10.1101/702654

Chen, X., Zheng, Y., Dong, C., & Song, S. (2021). Multi-dimensional enhanced seizure prediction framework based on graph convolutional network. *Frontiers in Neuroinformatics, 15*. https://doi.org/10.3389/fninf.2021.605729

Chu, H., Chung, C. K., Jeong, W., & Cho, K. H. (2017). Predicting epileptic seizures from scalp EEG based on attractor state analysis. *Computer Methods and Programs in Biomedicine, 143*, 75–87. https://doi.org/10.1016/J.CMPB.2017.03.002

Eftekhar, A., Juffali, W., El-Imad, J., Constandinou, T., & Toumazou, C. (2014). Ngram-derived pattern recognition for the detection and prediction of epileptic seizures. *PLoS One, 9*, Article e96235. https://doi.org/10.1371/journal.pone.0096235

Geng, M., Zhou, W., Liu, G., Li, C., & Zhang, Y. (2020). Epileptic seizure detection based on Stockwell transform and bidirectional long short-term memory. *IEEE Transactions on Neural Systems and Rehabilitation Engineering, 28*(3), 573–580. https://doi.org/10.1109/TNSRE.2020.2966290

Huang, G., Liu, Z., Van Der Maaten, L., & Weinberger, K. Q.. Densely connected convolutional networks [Online]. Available: https://github.com/liuzhuang13/DenseNet.

Jana, R., Bhattacharyya, S., & Das, S. (2019). Epileptic seizure prediction from EEG signals using DenseNet. In *2019 IEEE symposium series on computational intelligence (SSCI)* (pp. 604–609). https://doi.org/10.1109/SSCI44817.2019.9003059

Khan, H., Marcuse, L., Fields, M., Swann, K., & Yener, B. (2018). Focal onset seizure prediction using convolutional networks. *IEEE Transactions on Biomedical Engineering, 65*(9), 2109–2118. https://doi.org/10.1109/TBME.2017.2785401

Korff, C. M., Brunklaus, A., & Zuberi, S. M. (2015). Epileptic activity is a surrogate for an underlying etiology and stopping the activity has a limited impact on developmental outcome. *Epilepsia, 56*(10), 1477–1481. https://doi.org/10.1111/epi.13105

Lian, Q., et al. (2020). Learning graph in graph convolutional neural networks for robust seizure prediction. *Journal of Neural Engineering, 17*(3). https://doi.org/10.1088/1741-2552/ab909d

Liang, W., Pei, H., Cai, Q., & Wang, Y. (2020). Scalp EEG epileptogenic zone recognition and localization based on long-term recurrent convolutional network. *Neurocomputing, 396*, 569–576. https://doi.org/10.1016/j.neucom.2018.10.108

Li, Y., Liu, Y., Guo, Y. Z., Liao, X. F., Hu, B., & Yu, T. (2022). Spatio-temporal-spectral hierarchical graph convolutional network with semisupervised active learning for patient-specific seizure prediction. *IEEE Transactions on Cybernetics, 52*(11), 12189–12204. https://doi.org/10.1109/TCYB.2021.3071860

Ozcan, A. R., & Erturk, S. (2019). Seizure prediction in scalp EEG using 3D convolutional neural networks with an image-based approach. *IEEE Transactions on Neural Systems and Rehabilitation Engineering, 27*(11), 2284–2293. https://doi.org/10.1109/TNSRE.2019.2943707

Park, Y., Luo, L., Parhi, K. K., & Netoff, T. (2011). Seizure prediction with spectral power of EEG using cost-sensitive support vector machines. *Epilepsia, 52*(10), 1761–1770. https://doi.org/10.1111/j.1528-1167.2011.03138.x

Ryu, S., & Joe, I. (2021). A hybrid densenet-LSTM model for epileptic seizure prediction. *Applied Sciences, 11*(16). https://doi.org/10.3390/app11167661

Salamon, J., & Bello, J.P. (2017). Deep convolutional neural networks and data augmentation for environmental sound classification. IEEE Signal Processing Letters, vol. 24, no. 3, pp. 279-283, March 2017, doi: 10.1109/LSP.2017.2657381.

Saminu S, Xu G, Shuai Z, Abd El Kader I, Jabire AH, Ahmed YK, Karaye IA, Ahmad IS. (2021). A Recent Investigation on Detection and Classification of Epileptic Seizure Techniques Using EEG Signal. Brain Sci., May 20;11(5):668. doi: 10.3390/brainsci11050668.

Shahidi Zandi, A., Tafreshi, R., Javidan, M., & Dumont, G. A. (2013). Predicting epileptic seizures in scalp EEG based on a variational bayesian Gaussian mixture model of zero-crossing intervals. *IEEE Transactions on Biomedical Engineering, 60*(5), 1401–1413. https://doi.org/10.1109/TBME.2012.2237399

Sharif, B., & Jafari, A. H. (2017). Prediction of epileptic seizures from EEG using analysis of ictal rules on Poincaré plane. *Computer Methods and Programs in Biomedicine, 145*, 11–22. https://doi.org/10.1016/J.CMPB.2017.04.001

Shoeibi, A., et al. (2021). Epileptic seizures detection using deep learning techniques: A review. In *International journal of environmental research and public health, 18*MDPI. https://doi.org/10.3390/ijerph18115780, 11.

Stockwell, R. G., Mansinha, L., & Lowe, R. P. (1996). Localization of the complex spectrum: the S transform. *IEEE Transactions on Signal Processing, 44*(4), 998–1001. https://doi.org/10.1109/78.492555

Truong, N. D., et al. (2018). Convolutional neural networks for seizure prediction using intracranial and scalp electroencephalogram. *Neural Networks, 105*, 104–111. https://doi.org/10.1016/J.NEUNET.2018.04.018

Veisi, I., Pariz, N., & Karimpour, A. (2007). Fast and robust detection of epilepsy in noisy EEG signals using permutation entropy. In *Proceedings of the 7th IEEE international conference on bioinformatics and bioengineering* (pp. 200–203). BIBE. https://doi.org/10.1109/BIBE.2007.4375565.

Xu, G., Ren, T., Chen, Y., & Che, W. (2020). A one-dimensional CNN-LSTM model for epileptic seizure recognition using EEG signal analysis. *Frontiers in Neuroscience, 14*. https://doi.org/10.3389/fnins.2020.578126

Zeng, M., Zhang, X., Zhao, C., Lu, X., & Meng, Q. (2021). GRP-DNet: A gray recurrence plot-based densely connected convolutional network for classification of epileptiform EEG. *Journal of Neuroscience Methods, 347*. https://doi.org/10.1016/j.jneumeth.2020.108953

Zhang, Y., Guo, Y., Yang, P., Chen, W., & Lo, B. (2020). Epilepsy seizure prediction on EEG using common spatial pattern and convolutional neural network. *IEEE Journal of Biomedical and Health Informatics, 24*(2), 465–474. https://doi.org/10.1109/JBHI.2019.2933046

Zhao, Y., et al. (2021). EEG-Based Seizure detection using linear graph convolution network with focal loss. *Computer Methods and Programs in Biomedicine, 208*, Article 106277. https://doi.org/10.1016/J.CMPB.2021.106277

Shoeb, A.H., & Guttag, J.V. (2010). Application of Machine Learning To Epileptic Seizure Detection. Proceedings of the 27th International Conference on Machine Learning (ICML-10), Pages 975–982, June 21-24, 2010, Haifa, Israel.

Navarin, N.O., Erb, W., Pasa, L., and Sperduti, A., *Linear Graph Convolutional Networks*. [Online]. Available: http://www.i6doc.com/en/.